

Photoemission studies of metals by using Mathieu potential

B Zoliana¹, Zaithanzauva Pachuau¹, Lalthakimi Zadeng, P K Patra², D T Khathing³ and R K Thapa*

Condensed Matter Theory Research Group, Department of Physics, Pachhunga University College, Mizoram University,
Aizawl, Mizoram-796 001, India

¹Department of Physics, Govt Ziri Residential Science College, Aizawl, Mizoram-796 001, India

²Science Education Centre, North-Eastern Hill University, Shillong-793 003, Meghalay, India

³Department of Physics, North-Eastern Hill University, Shillong-793 022, Meghalay, India

E-mail: rkt@sancharnet.in

Received 25 February 2003, accepted 7 March 2003

Abstract : Photocurrent results from ferromagnetic materials Fe and Ni and *d*-band metals Pd and Cr is discussed which is calculated by using the Mathieu potential for the crystal. A local dielectric functions have been used to calculate the electromagnetic field for the bulk, surface and vacuum regions of the metals.

Keywords : Photoemission, metals, Mathieu potential

PACS Nos. : 79.60.Bm, 77.22.Ch

Mathieu potential had been applied to photoemission calculations by Pachuau *et al* [1] in the case of empty potential and a strong potential [2]. These cases had been applied to free-electron type metals like Al and Be for empty potentials and *d*-band type metals Cu, W, Mo and also Si. It has been seen that surface photoeffect had been exhibited in these metals for values of incident photon energies below and above the plasmon energy but within low photon energy range. With this view in mind, we present in this Note, the extension of Mathieu potential model developed to the calculations of photocurrent from ferromagnetic metals Ni and Fe and transition metals Pd and Cr.

The photocurrent density formula [1] from golden rule approximation can be written as

$$\frac{dj(E)}{d\Omega} = \frac{2\pi}{\hbar} \sum_i |\langle \psi_f | H' | \psi_i \rangle|^2 \delta(E - E_f) \times \delta(E_f - E_i - \hbar\omega) f_0(E - \hbar\omega) [1 - f_0(E)], \quad (1)$$

where $\psi_i, (\psi_f)$ refer to the initial (final) state wavefunctions, perturbation H' can be written as

$$H' = \frac{1}{2m_e c} (\mathbf{A} \cdot \mathbf{p} + \mathbf{p} \cdot \mathbf{A}),$$

where m_e is the mass of the electron, \mathbf{p} the one-electron momentum operator and \mathbf{A} is the vector potential of the incident photon field. With simple modifications, the photon field used in our calculations for three regions can be written as

$$\tilde{A}_\omega(\omega, x) = \begin{cases} A_1, & x < -d \quad (\text{bulk}), \\ \frac{A_1 \cdot \epsilon(\omega) \cdot d}{[1 - \epsilon(\omega)]x + d}, & -d \leq x \leq 0 \quad (\text{surface}), \\ A_1 \cdot \epsilon(\omega), & x \geq 0 \quad (\text{vacuum}), \end{cases} \quad (2)$$

where A_1 is a constant depending on the dielectric function $\epsilon(\omega)$, photon energy $\hbar\omega$ and angle of incidence θ . $\epsilon(\omega)$ is defined locally and interpolates linearly between the bulk

*Corresponding Author

and the vacuum values. Considering one-dimensional crystal, its potential is represented by $V(x) = V_a \cos 2\pi x/a$, where a is the period of the crystal potential and maximum (repulsive) value is V_a at $x = 0$. The one dimensional Schrodinger's equation can now be written as

$$\frac{d^2\psi}{dz^2} + (a2q \cos 2z)\psi = 0, \quad (3)$$

where $2q = \frac{V_a}{a}$, $\tau = \frac{\pi x}{a}$, $T = \frac{\pi}{a}$, $a = \frac{E}{T}$. Here, q is the magnitude of the potential which measured its strength. Eq. (3) can be solved for obtaining initial state wavefunction $\psi_i(x)$ for the bulk and surface regions ($x \leq 0$) and also for the vacuum regions. These wavefunctions as derived are given by (in atomic units) :

$$\psi_i(x, q) = \begin{cases} 4\pi k_i^{1/2} \left(1 - \frac{q}{16} + \frac{11}{64}q^2\right) e^{-\mu(\lambda'_0 - x)}, & x \leq x'_0, \\ (2\zeta)^{1/2} e^{-\xi(x - x'_0)}, & x > x'_0. \end{cases} \quad (4)$$

The derivation of $\psi_i(x, q)$ had been discussed in detail by Pachau [2,3]

The step potential at the surface encountered by an electron is defined by $V(x) = -V_0\theta(x)$, where $\theta(x)$ is unit function such that $\theta(x) = 1(0)$ for $x > 0$ ($x < 0$). The final state wavefunction which is the solution of this step potential and is given by (in atomic units) :

$$\psi_f(x) = \begin{cases} 2\pi q_f \left(\frac{2q_f}{q_f + k_f} e^{ik_f x} e^{-\alpha|x|}, \right. & x < 0 \text{ (bulk and surface),} \\ \left. 2\pi q_f \left(\frac{q_f - k_f}{q_f + k_f} \right) e^{-iq_f x} \right) & x > 0 \text{ (vacuum),} \end{cases} \quad (5)$$

where $k_f^2 = 2E_f$, $q_f^2 = 2(E_f - V_0)$ and $E_f = E_i + \hbar\omega$

In eq. (5), the factor $e^{-\alpha|x|}$ is included on the surface and bulk side to take into account the inelastic scattering of the electrons.

Photocurrent was calculated from metals Fe, Ni, Pd and Cr as a function of incident photon energy ($\hbar\omega$) for two different values of surface width $d = 10$ a.u. and $d = 0.0$. The real and imaginary parts of dielectric constants were calculated for each of these metals by using the experimentally determined values [4] of refractive indices and absorption coefficients (extinction constant). However, we have used the same surface parameters E_i, θ, \dots , for all the metals as was used in the case of Cu.

Referring to Figure 1, we have plotted photocurrent as a function of photon energy ($\hbar\omega$) in the case of Fe. It is

observed that maximum in photocurrent is obtained at $\hbar\omega = 15$ eV for $d = 10$ a.u. For further increase in photon energy, photocurrent decreases and becomes minimum at $\hbar\omega = 19$ eV. A second peak of small height in photocurrent is obtained at $\hbar\omega = 24$ eV. Similarly in the case of Ni also,

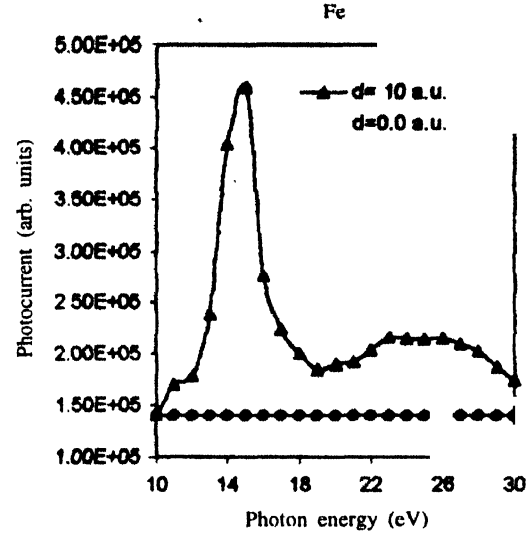


Figure 1. Variation of photocurrent against photon energy for surface width $d = 10.0$ a.u. and narrow surface width ($d = 0.0$ a.u.) in the case of Fe

we have plotted (Figure 2) photocurrent as a function of photon energy for $d = 10$ a.u. For Ni, we find a maximum in photocurrent at photon energy $\hbar\omega = 15$ eV, but it decreases towards zero as photon energy is further increased

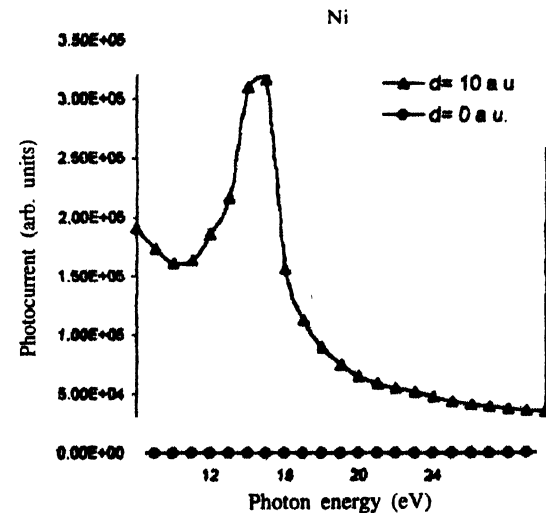


Figure 2. Same as in Figure 1 in the case of Ni.

Besides these two magnetic metals, photocurrent was also calculated in the case of Pd and Cr with the same initial parameters as was used in the case of Fe and Ni. The behaviour of photocurrent is shown in Figure 3. For surface width $d = 10$ a.u., we find that a maximum in photocurrent occurred at $\hbar\omega = 8$ eV, decreased to minimum at

$\hbar\omega = 15$ eV. It showed a small hump in photocurrent for $\hbar\omega = 17$ eV and decreased to minimum again for further increase of photon energy. Photocurrent data of Pd showed behaviour exactly similar to that obtained by Thapa [5] but by using the Kronig-Penney potential model. For narrow surface width, photocurrent data showed a constant value also for Pd when plotted against photon energy.

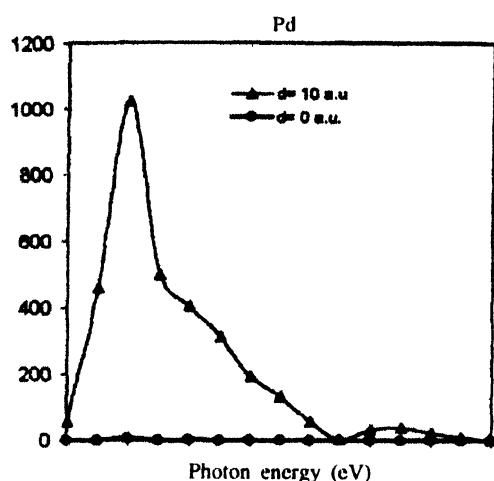


Figure 3. Same as in Figure 1 in the case of Pd.

We show in Figure 4, the plot of photocurrent as a function of photon energy in the case of Cr. For $d = 10$ a.u., there is a peak in photocurrent obtained at $\hbar\omega = 14$ eV. Again, photocurrent decreased to minimum at $\hbar\omega = 19$ eV and showed a second hump of lower magnitude at $\hbar\omega = 27$ eV. Cr also showed similar behaviour for narrow surface width as seen in the case of Fe, Ni and Pd.

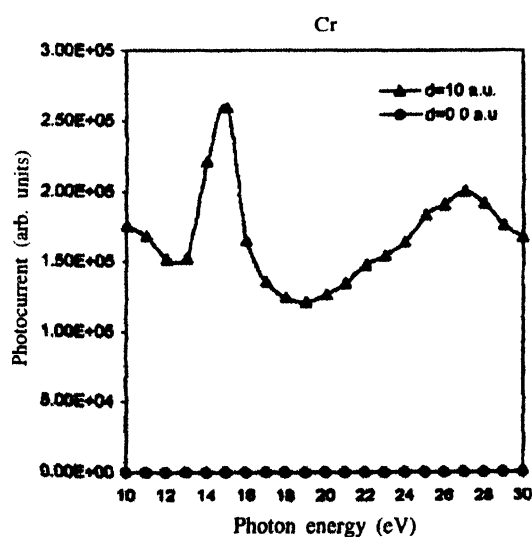


Figure 4. Same as in Figure 1 in the case of Cr.

We find from our results that in the low photon energy range all the metals showed similar trends in the behaviour of photocurrent for both the surface widths. The origin of first peak at $\hbar\omega = 8$ eV in the case of Pd is attributed to

surface photoeffect as explained by Thapa [5]. This had been evidenced by the plot of field for photon energy below and above 8 eV. The decrease in photocurrent to minimum after the first peak in all the metals is due to loss of photon energy by excitations of bulk plasmons. Plasmons in metals and semiconductors play a significant role in transport and optical properties. Surface plasmons and in general, the dynamical screen properties at the surface attracted therefore considerable attention [6,7]. Surface plasmons in particular, are of importance as it is linked to the position of the centroid of the screening charge [8] at the surface plasmon frequency. We assume the surface plasmon frequency (ω_s) to be the value of photon frequency at which photocurrent is maximum and this is related to bulk plasmon frequency (ω_B) by $\omega_s \approx \omega_B \sqrt{2}$. Further, it had been already shown from electrodynamics of surface phenomena [9] that at frequency $\omega \approx \omega_B$, the component of electromagnetic field (vector potential) tends towards minimum which causes the photocurrent to be also minimum. We find that the metals under study, satisfy this condition although bulk plasmon frequency (energy) is not a well-defined quantity. Here, we have considered it to be equal to the value at which $\epsilon_1 \rightarrow 0$.

We have also plotted photocurrent as a function of $\hbar\omega$ for narrow surface width i.e. $d = 0$ a.u. by including Fresnel fields for all the metals under study. The behaviour of photocurrent in this case, was found to be quite different. There is no peak in photocurrent found as in the case for $d = 10$ a.u. The photocurrent in this case, is constant and remains parallel with the x-axis. This indicates that inclusion of field is important in photoemission calculations.

We have tried in this report to see the effect of Mathieu type of potential on photoemission calculations. We find that photocurrent results from these metals showed similar behaviour as had been obtained by Thapa *et al* [10] in the case of other metals and semiconductors [11]. However, the main drawback of the model presented here is that the same initial state wavefunction is used both for the surface and the bulk regions of the metal to calculate the photocurrent. We are working to represent the initial state wavefunction accurately for these regions by applying the projection operator method of group theory [12].

Acknowledgments

RKT and PKP thanks University Grants Commission, New Delhi for a research grant. Prof. S G Davison and Prue Davison, Department of Applied Mathematics and Physics, University of Waterloo, Ontario, Canada, have helped with many relevant literature connected with the works reported here.

References

- [1] Z Pachuau, B Zoliana, D T Khating, P K Patra and R K Thapa, *Phys. Lett. A* **275** 459 (2000)
- [2] Zaithanzauva Pachuau, B Zoliana, P K Patra, D T Khating and R K Thapa *Phys. Lett. A* **294** 52 (2002)
- [3] Zaithanzauva Pachuau *PhD Thesis* (unpublished) (North-Eastern Hill University, Shillong, India)
- [4] J Weaver *Handbook of Chemistry and Physics* (Boca Raton : CRC Press) (1987)
- [5] R K Thapa *Phys. Stat. Sol.* **B179** 391 (1993)
- [6] P J Feibelman *Prog. Surf. Sci.* **12** 287 (1982)
- [7] P Apell, A Ljungbert and S Lundqvist *Phys. Scripta* **30** 367 (1984)
- [8] M Rocca and F Moresco *Prog. Surf. Sci.* **53** 331 (1996)
- [9] Zaithanzauva Pachuau, B Zoliana, P K Patra and R K Thapa *3rd Regional Conference on Physics Research in North-East* (Dibrugarh University, Dibrugarh, India, 9th November 2002)
- [10] R K Thapa and N Kar *Phys. Rev.* **B51** 17980 (1995)
- [11] R K Thapa and N Kar *Mod. Phys. Lett.* **B8** 361 (1994)
- [12] B Zoliana, Zaithanzauva Pachuau, P K Patra, D T Khating and R K Thapa *3rd Regional Conference on Physics Research in North-East* (Dibrugarh University, Dibrugarh, India, 9th November 2002); B Zoliana, Z Pachuau, R K Thapa, Lalthakimi Zadeng, P K Patra and D T Khating *Intl. J. Mod. Phys. B* (accepted)